

## Molecular Imaging of Cancer with Copper-64 Radiopharmaceuticals and Positron Emission Tomography (PET)

MONICA SHOKEEN<sup>†</sup> AND CAROLYN J. ANDERSON<sup>\*,†,‡,§</sup>

<sup>†</sup>Mallinckrodt Institute of Radiology, <sup>‡</sup>Department of Biochemistry, Washington University School of Medicine, St. Louis, Missouri 63110, <sup>§</sup>Department of Chemistry, Washington University, St. Louis, Missouri 63130

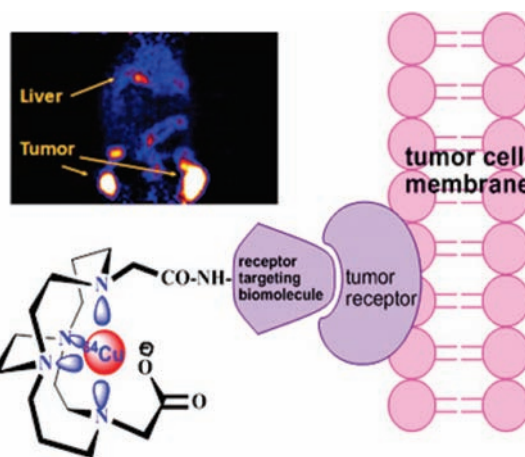
RECEIVED ON NOVEMBER 14, 2008

### CONSPECTUS

Molecular imaging has evolved over the past several years into an important tool for diagnosing, understanding, and monitoring disease. Molecular imaging has distinguished itself as an interdisciplinary field, with contributions from chemistry, biology, physics, and medicine. The cross-disciplinary impetus has led to significant achievements, such as the development of more sensitive imaging instruments and robust, safer radiopharmaceuticals, thereby providing more choices to fit personalized medical needs. Molecular imaging is making steadfast progress in the field of cancer research among others. Cancer is a challenging disease, characterized by heterogeneity, uncontrolled cell division, and the ability of cancer cells to invade other tissues. Researchers are addressing these challenges by aggressively identifying and studying key cancer-specific biomarkers such as growth factor receptors, protein kinases, cell adhesion molecules, and proteases, as well as cancer-related biological processes such as hypoxia, apoptosis, and angiogenesis.

Positron emission tomography (PET) is widely used by clinicians in the United States as a diagnostic molecular imaging tool. Small-animal PET systems that can image rodents and generate reconstructed images in a noninvasive manner (with a resolution as low as 1 mm) have been developed and are used frequently, facilitating radiopharmaceutical development and drug discovery. Currently, [<sup>18</sup>F]-labeled 2-fluorodeoxyglucose (FDG) is the only PET radiotracer used for routine clinical evaluation (primarily for oncological imaging).

There is now increasing interest in nontraditional positron-emitting radionuclides, particularly those of the transition metals, for imaging with PET because of increased production and availability. Copper-based radionuclides are currently being extensively evaluated because they offer a varying range of half-lives and positron energies. For example, the half-life (12.7 h) and decay properties ( $\beta^+$ , 0.653 MeV, 17.8%;  $\beta^-$ , 0.579 MeV, 38.4 %; the remainder is electron capture) of <sup>64</sup>Cu make it an ideal radioisotope for PET imaging and radiotherapy. In addition, the well-established coordination chemistry of copper allows for its reaction with a wide variety of chelator systems that can potentially be linked to antibodies, proteins, peptides, and other biologically relevant molecules. New chelators with greater *in vivo* stability, such as the cross-bridged (CB) versions of tetraazamacrocyclic 1,4,8,11-tetraazacyclotetradecane-1,4,8,11-tetraacetic acid (TETA), are now available. Finally, one of the major aspects of successful imaging is the identification and characterization of a relevant disease biomarker at the cellular and subcellular level and the ensuing development of a highly specific targeting moiety. In this Account, we discuss specific examples of PET imaging with new and improved <sup>64</sup>Cu-based radiopharmaceuticals, highlighting the study of some of the key cancer biomarkers, such as epidermal growth-factor receptor (EGFR), somatostatin receptors (SSRs), and integrin  $\alpha_v\beta_3$ .



## Molecular Imaging with Positron Emission Tomography (PET)

PET requires the injection of molecules labeled with radionuclides (radiopharmaceuticals) into the subject for obtaining an image. The amount of material that is injected into the subject is extremely small (at the level of nanomoles to picomoles) and causes minimal pharmacological effect. In this regard, PET enables the imaging and monitoring of disease in a noninvasive manner. PET has become a widely used diagnostic imaging tool by clinicians in the United States with 1.52 million PET and PET/CT imaging procedures performed in 2008, compared with 1.46 million scans performed in 2007 ([http://www.molecularimaging.net/index.php?option=com\\_articles&view=article&id=16290](http://www.molecularimaging.net/index.php?option=com_articles&view=article&id=16290)). Although there have been thousands of radiopharmaceuticals developed for potential use in a clinical imaging setting, at present, [ $^{18}\text{F}$ ]-labeled 2-fluorodeoxyglucose (FDG) is the only PET radiotracer used for routine clinical evaluation, primarily for oncological imaging. The underlying mechanism for generating a PET image is depicted in Figure 1.

Nontraditional positron-emitting radionuclides, particularly those of the transition metals, have gained considerable interest for imaging with PET because of increased production and availability. Significant research effort has been devoted to  $^{64}\text{Cu}$  because of its longer half-life (12.7 h) and decay properties ( $\beta^+$ , 0.653 MeV [17.8%];  $\beta^-$ , 0.579 MeV [38.4%]). In addition, the well-established coordination chemistry of copper allows for its reaction with a wide variety of chelator systems that can potentially be linked to antibodies, proteins, peptides, and other biologically relevant molecules. This Account will discuss the chemistry of developing  $^{64}\text{Cu}$  radiopharmaceuticals and their applications in the molecular imaging of cancer.

## Coordination Chemistry of Copper

The aqueous coordination chemistry of copper is limited to its three accessible oxidation states (I–III).<sup>1,2</sup> The lowest oxidation state, Cu(I), has a diamagnetic  $d^{10}$  configuration and forms complexes without any crystal-field stabilization energy. Complexes of this type are readily prepared using relatively soft polarizable ligands like thioethers, phosphines, nitriles, isonitriles, iodide, cyanide, and thiolates; however, Cu(I) complexes are typically not used for *in vivo* imaging due to their lability. Copper(II) is a  $d^9$  metal of borderline softness, which favors amines, imines, and bidentate ligands like bipyridine to form square-planar, distorted square-planar, trigonal-pyramidal, square-pyramidal, and distorted octahedral geometries. Jahn–Teller distortions in six-coordinate Cu(II) complexes are

often observed as an axial elongation or a tetragonal compression. Due to the presence of some crystal-field stabilization energy, Cu(II) is generally less labile toward ligand exchange compared with Cu(I) and in our opinion is the best candidate for incorporation into radiopharmaceuticals. A third oxidation state, Cu(III), is relatively rare and difficult to attain without the use of strong  $\pi$ -donating ligands.

## Production of $^{64}\text{Cu}$

Copper-64 can be effectively produced by both reactor-based and accelerator-based methods. One method of  $^{64}\text{Cu}$  production is the  $^{64}\text{Zn}(n,p)^{64}\text{Cu}$  reaction in a nuclear reactor.<sup>3</sup> Most reactor-produced radionuclides are produced using thermal neutron reactions, or  $(n,\gamma)$  reactions, where the thermal neutron is of relatively low energy and the target material is of the same element as the product radionuclide. For producing high-specific activity  $^{64}\text{Cu}$ , fast neutrons are used to bombard a natural Zn target in an  $(n,p)$  reaction. This method enabled the production of high specific activity  $^{64}\text{Cu}$  at the Missouri University Research Reactor (MURR) in amounts averaging 9.25 GBq (250 mCi).<sup>3</sup> Unfortunately, one of the byproducts of producing  $^{64}\text{Cu}$  with a natural Zn target was  $^{65}\text{Zn}$  ( $T_{1/2} = 245$  d), which limits the practicality of production by this method.

The production of no-carrier-added  $^{64}\text{Cu}$  via the  $^{64}\text{Ni}(p,n)^{64}\text{Cu}$  reaction on a biomedical cyclotron was proposed by Szelecsenyi et al.<sup>4</sup> In this study, small irradiations were performed demonstrating the feasibility of  $^{64}\text{Cu}$  production by this method.<sup>4</sup> Subsequent studies by McCarthy et al. were performed, and this method is now used to provide  $^{64}\text{Cu}$  to researchers throughout the United States.<sup>5</sup>

## Chelating Ligands for $^{64}\text{Cu}$

High specific activity  $^{64}\text{Cu}$  with a chelator that forms highly stable complexes *in vivo* is critical for achieving high uptake of  $^{64}\text{Cu}$  in the target tissue while minimizing non-target-tissue uptake. Ligands that can form  $^{64}\text{Cu}$  complexes with high kinetic inertness to Cu(II) decomplexation (proton-assisted as well as transchelation or transmetalation) are ideal, since this is more significant than thermodynamic stability after the  $^{64}\text{Cu}$  complex is injected into a living organism.<sup>6,7</sup> Reduction of Cu(II) to Cu(I) and subsequent Cu(I) loss may also be a pathway for loss of  $^{64}\text{Cu}$ , and resistance of the  $^{64}\text{Cu}$  complex to Cu(II)/Cu(I) reduction as well as reversibility can also be important.<sup>8</sup> Rapid complexation kinetics are also essential to allow for the facile formation of the  $^{64}\text{Cu}$  complex. Finally, chelators also must be designed with available functional groups

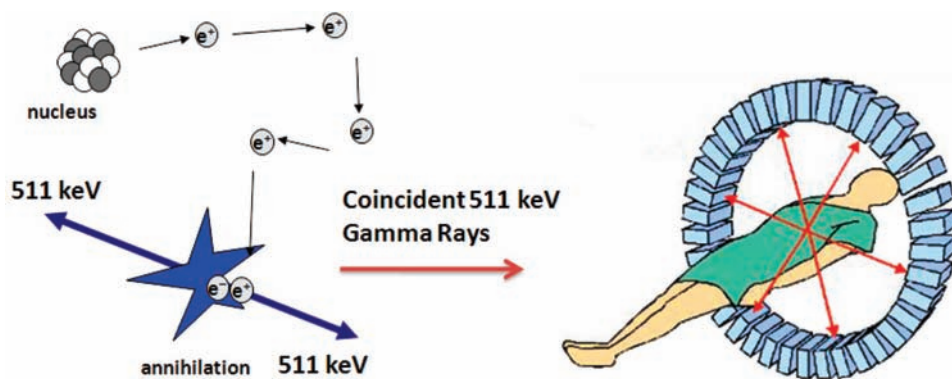


**FIGURE 1.** Schematic of imaging with positron emission tomography (PET). The positron travels away from its origin and then collides with a negatively charged electron in tissue, producing annihilation radiation of two 511 keV photons approximately 180° apart. These coincident emissions are detected by the PET scanner.

that allow them to be covalently linked to targeting peptides, proteins, and antibodies.

## Chelators Based on Cyclam and Cyclen Backbones

The most widely used chelators for attaching  $^{64}\text{Cu}$  to biological molecules are tetraazamacrocyclic ligands with pendant arms that utilize both the macrocyclic and chelate effects to enhance stability. By far the most extensively used class of chelators for  $^{64}\text{Cu}$  has been the macrocyclic polyaminocarboxylates shown in Figure 2. These systems have been thoroughly investigated, and *in vitro* and *in vivo* testing have shown them to be superior to acyclic chelating agents for  $^{64}\text{Cu}$ .<sup>6</sup> This enhanced stability is most likely due to the greater geometrical constraint incorporated into the macrocyclic ligand that enhances the kinetic inertness and thermodynamic stability of their  $^{64}\text{Cu}$  complexes.<sup>9,10</sup> Two of the most important chelators studied were 1,4,7,10-tetraazacyclododecane-1,4,7,10-tetraacetic acid (DOTA) and 1,4,8,11-tetraazacyclotetradecane-1,4,8,11-tetraacetic acid (TETA). While DOTA has been used as a bifunctional chelator (BFC) for  $^{64}\text{Cu}$ , its ability to bind many different metal ions, and its decreased stability compared with TETA make it less than ideal.<sup>11–13</sup> The tetraazamacrocyclic ligand TETA, therefore, has been extensively used as a chelator for  $^{64}\text{Cu}$ , and successful derivatization of this ligand has allowed researchers to conjugate it to antibodies, proteins, and peptides.<sup>14–16</sup>

Although  $^{64}\text{Cu}$ -TETA complexes are more stable than  $^{64}\text{Cu}$ -DOTA and  $^{64}\text{Cu}$ -labeled complexes of acyclic ligands, their instability *in vivo* has been well documented. Bass et al. demonstrated that when  $^{64}\text{Cu}$ -TETA-octreotide (OC) was injected into normal Sprague–Dawley rats, nearly 70% of the  $^{64}\text{Cu}$  from  $^{64}\text{Cu}$ -TETA-OC was transchelated to a 35 kDa species believed to be superoxide dismutase (SOD) in the liver 20 h

postinjection.<sup>17</sup> These results are supported by the observations of Boswell et al.<sup>7</sup>

Despite the considerable efforts made by researchers to use tetraaza-tetracarboxylate macrocyclic ligands as effective BFCs for  $^{64}\text{Cu}$ , it is evident that the *in vivo* instability of these  $^{64}\text{Cu}$  complexes emphasizes the need for more inert  $^{64}\text{Cu}$  chelators. With this goal, new ligand systems, including those based upon the cross-bridged (CB) tetraazamacrocycles have been developed to complex  $^{64}\text{Cu}$  more stably.

## The Cross-Bridged Tetraamine Ligands

This class of chelators was first conceived of and synthesized by Weisman, Wong, and co-workers in the 1990s,<sup>18,19</sup> and they were originally designed to complex metal cations like  $\text{Li}^+$ ,  $\text{Cu}^{2+}$ , and  $\text{Zn}^{2+}$  within their clamshell-like clefts. Numerous copper complexes of these and related ligands have since been prepared and studied by the Wong and Weisman laboratories as well as other research groups.<sup>20–22</sup> With the available structural data, the expected *cis*-folded coordination geometry of these chelators has been confirmed in all cases. Attachment of two carboxymethyl pendant arms to CB-cyclam to give CB-4,11-bis(carboxymethyl)-1,4,8,11-tetraazabicyclo[6.6.2]hexadecane (TE2A) further ensures complete envelopment of a six-coordinate Cu(II) as shown in Figure 2.

While the measurement of stability constants of Cu(II)-CB complexes has been limited by the proton-sponge nature of these chelators, available data for Cu(II)-CB-cyclam ( $\log K_f = 27.1$ ) revealed very similar values to nonbridged Cu(II)-cyclam ( $\log K_f = 27.2$ ) and related complexes.<sup>23</sup> On the other hand, their kinetic inertness, especially in aqueous solution, has been shown to be truly exceptional.<sup>8,24</sup> Proton-assisted decomplexation is one indicator of solution inertness. Under pseudo-first-order conditions of high acid concentration (e.g., 5 M HCl), decomplexation half-lives can

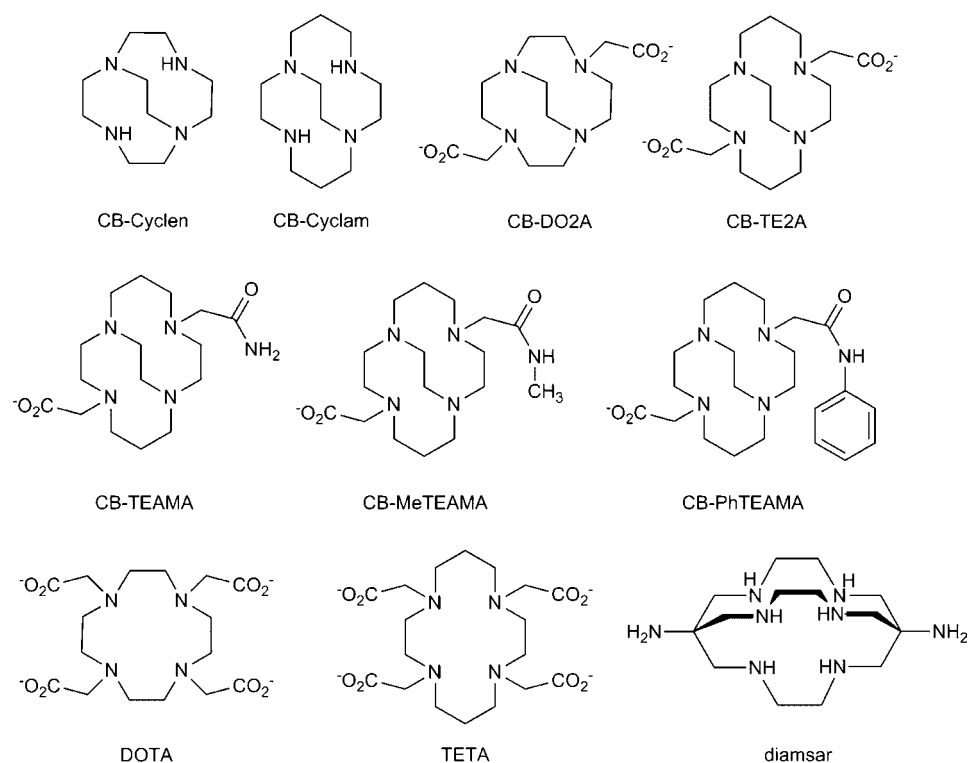


**FIGURE 2.** Selected macrocyclic chelators that have been investigated for chelating copper radionuclides.

**TABLE 1.** Pseudo-First-Order Half-Lives for Acid Decomplexation and Reduction Potentials of Cu(II) Complexes<sup>a</sup>

chelator	5 M HCl, 90 °C	12 M HCl, 90 °C	$E_{\text{red}}$ (V) vs Ag/AgCl
DOTA	<3 min	<3 min	-0.94 (irrev) <sup>b</sup>
cyclam	<3 min	<3 min	-0.68 (quasi-rev)
TETA	4.5(5) min	<3 min	-1.18 (irrev)
CB-cyclam	11.7(1) min	<3 min	-0.52 (quasi-rev)
CB-TE2A	154(6) h	1.6(2) h	-1.08 (quasi-rev)
CB-DO2A	<3 min	nd	-0.92 (irrev)
CB-TEAMA	nd	nd	-0.96 (quasi-rev)
diamsar	40(1) h	<3 min	-1.1 (irrev)

<sup>a</sup> All values are from Heroux et al.<sup>24</sup> unless otherwise noted. <sup>b</sup> Reference 7.

provide a comparative gauge. Remarkable resistance of Cu-CB complexes toward such processes has recently been demonstrated.<sup>8,24</sup> As shown in Table 1, Cu-CB-cyclam is almost an order of magnitude more inert than Cu(II)-cyclam in 5 M HCl at 90 °C, while Cu(II)-CB-TE2A is 4 orders of magnitude more inert. Impressively, the latter complex resists acid decomplexation even better than the fully encapsulated sarcophagine complex Cu(II)-3,6,10,13,16,19-hexaazabicyclo[6.6.6]heptacosane-1,8-diamine (diamsar). It was confirmed that both the cross-bridged cyclam backbone and the presence of two enveloping carboxymethyl arms are required for this unusual kinetic inertness.

Biological stability of  $^{64}\text{Cu}$ -labeled cross-bridged complexes, including CB-cyclam,  $^{64}\text{Cu}$ -CB-TE2A, and CB-10-bis(carboxymethyl)-1,4,7,10-tetraazabicyclo[5.5.2]tetra-

decane (DO2A), has been investigated.<sup>7,23</sup> The biodistribution of these  $^{64}\text{Cu}$  complexes in female Sprague–Dawley rats was highly dependent upon the chelator. Based on the rapid clearance from blood, liver, and kidney,  $^{64}\text{Cu}$ -CB-TE2A was thought to be the most stable (Figure 3).<sup>23</sup> Follow-up metabolism studies of  $^{64}\text{Cu}$ -CB-TE2A and  $^{64}\text{Cu}$ -CB-DO2A compared with  $^{64}\text{Cu}$ -DOTA and  $^{64}\text{Cu}$ -TETA demonstrated the robust stability of  $^{64}\text{Cu}$ -CB-TE2A *in vivo*, with low amounts of transchelation to liver and blood proteins.<sup>7</sup>

## Selection of Biological Targets of Disease for Molecular Imaging

The selection of right target/biomarker has been greatly enhanced by the improved fundamental understanding of various aspects of cellular functioning. The target could be a surface protein/integrin or an intracellular component such as DNA, mRNA, or cytoplasmic protein (Figure 4). Surface proteins are easier to target, because the targeting ligand does not have to gain access to the inside the diseased cell. Another key factor in target selection is the number of target sites in the diseased cell. Choosing an abundant target will make imaging more feasible.

Imaging markers, such as a labeled antibody, peptide, or peptidomimetic, can be used to reach the target to serve an imaging or therapeutic purpose. In the case of a surface

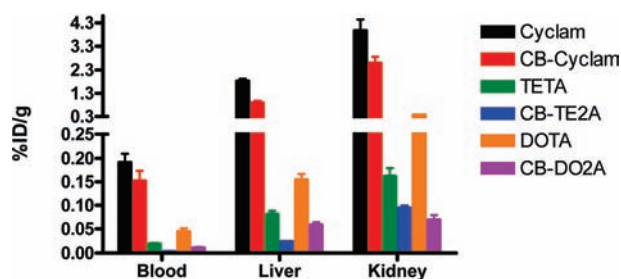


**FIGURE 3.** Biodistribution data of selected  $^{64}\text{Cu}$ -labeled cyclam and bridged cyclam analogs at 24 h postinjection (pi) in normal rats. Adapted from refs 7, 23, and 45.

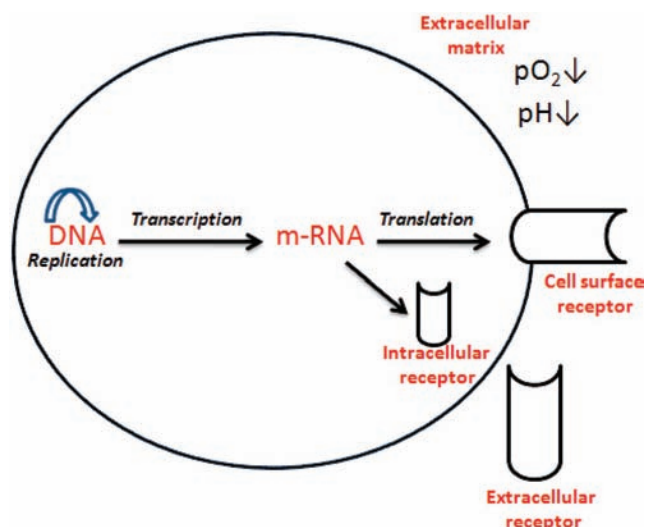


**FIGURE 4.** Simplified Schematic of a tumor cell showing the various intracellular, cell surface, and extracellular targets available for molecular imaging.

protein target, the targeting unit should be able to bind competitively to the target with an affinity comparable to or better than the natural binding ligand, thereby inhibiting the binding of the activating (natural) ligand to the receptor. Some of the cell surface proteins that our laboratory has investigated include epidermal growth-factor receptor (EGFR), somatostatin receptors (SSRs), and integrin  $\alpha_v\beta_3$ . Select studies on some of these targets are covered in the following sections.

### Targeting Somatostatin Receptors (SSRs)

Somatostatin is a 14 amino acid peptide that is involved in the regulation and release of a number of hormones, and SSRs are present in many different normal organ systems such as the central nervous system (CNS), the gastrointestinal tract, and the exocrine and endocrine pancreas. Several human tumors of the neuroendocrine system, CNS, breast, and lung are SSR positive, making it a viable disease target. An eight amino acid analog of somatostatin, octreotide (OC) has a longer biological half-life and is shown to be several times

more effective than somatostatin in the suppression of growth hormone secretion in animals.<sup>25</sup> Somatostatin analogs that have been conjugated with various metal chelators and labeled with  $^{111}\text{In}$  or  $^{64}\text{Cu}$  for evaluating somatostatin receptor positive tumors in rodent models and humans are represented in Figure 5.

In one of our earlier studies with SSRs, we conducted *in vitro* and *in vivo* evaluation of  $^{64}\text{Cu}$ -labeled OC conjugates.<sup>15</sup> OC was conjugated with TETA for labeling with  $^{64}\text{Cu}$ , and this agent was compared with  $^{111}\text{In}$ -DTPA-D-Phe<sup>1</sup>-OC ( $^{111}\text{In}$ -DTPA-OC; Octreoscan), a SPECT imaging agent approved for routine clinical use as a diagnostic agent for neuroendocrine cancer in the US and Europe.<sup>26</sup>  $^{64}\text{Cu}$ -TETA-OC was evaluated as a PET imaging agent in humans (eight subjects) and compared with  $^{111}\text{In}$ -DTPA-OC with gamma scintigraphy and SPECT imaging.<sup>27</sup>  $^{64}\text{Cu}$ -TETA-OC and PET imaged more tumors in two patients compared with  $^{111}\text{In}$ -DTPA-OC and SPECT, and in one patient  $^{111}\text{In}$ -DTPA-OC and SPECT weakly imaged a lung lesion that was not detected with  $^{64}\text{Cu}$ -TETA-OC. Overall,  $^{64}\text{Cu}$ -TETA-OC and PET showed greater sensitivity for imaging neuroendocrine tumors, in part due to the greater sensitivity of PET compared with SPECT.

*In vitro* and *in vivo* evaluation of a second generation somatostatin analog,  $^{64}\text{Cu}$ -TETA-Y3-TATE (Y3-TATE = tyrosine-3-octreotate) was conducted. Y3-TATE differs from OC in that tyrosine replaces phenylalanine in the 3-position, and the C-terminal threonine is an acid rather than an alcohol and has shown improved targeting of somatostatin-rich tissues.<sup>28,29</sup>  $^{64}\text{Cu}$ -TETA-Y3-TATE had high binding affinity to somatostatin in receptor-positive CA20948 rat pancreatic tumor cell membranes. *In vivo*, in CA20948 and AR42J rat pancreatic tumor models,  $^{64}\text{Cu}$ -TETA-Y3-TATE had twice as much uptake as  $^{64}\text{Cu}$ -TETA-OC. This new reagent demonstrated superior potential as a radiopharmaceutical for imaging and therapy of SSR-positive tissues.

From a synthetic point of view, it was a worthwhile prospect to evaluate which chemical modification in the structure led to the increased uptake in somatostatin-rich tissues *in vivo*: was it due to the C-terminal carboxylate or the substitution of tyrosine for phenylalanine at the 3-position? These issues were addressed in a study where four  $^{64}\text{Cu}$ -labeled somatostatin analogues were compared *in vitro* and in a tumor-bearing rat model.<sup>28</sup> The effect of single modifications to the OC peptide on target tissue uptake was investigated. In particular, two new modifications of the OC peptide were synthesized: one with the substitution of the tyrosine for phenylalanine in the 3-position (Y3-OC), and

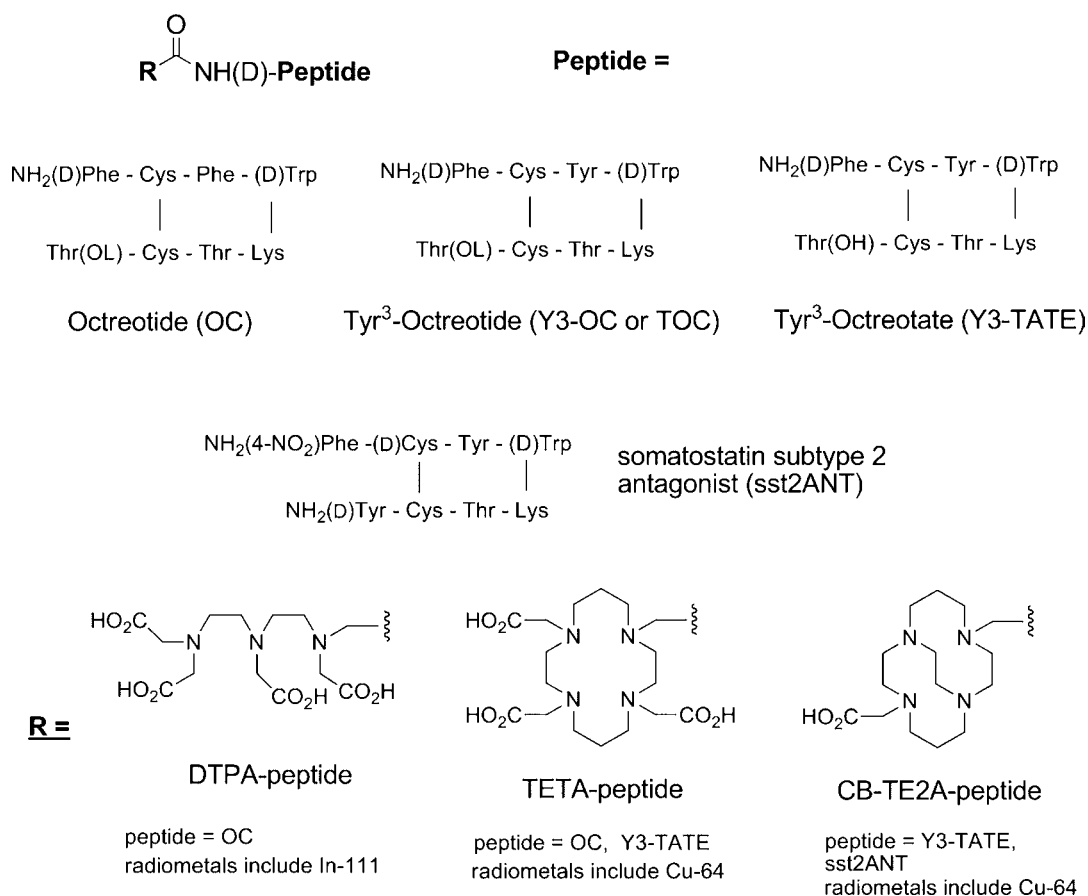


**FIGURE 5.** Somatostatin analogs that have been conjugated with various metal chelators and labeled with  $^{111}\text{In}$  or  $^{64}\text{Cu}$  for evaluating somatostatin receptor positive tumors in rodent models and humans.

other changing the C-terminus from an alcohol to a carboxylic acid (TATE). Both of these peptides were conjugated with TETA for labeling with  $^{64}\text{Cu}$ . The *in vitro* and *in vivo* behaviors of these two peptides were compared with  $^{64}\text{Cu}$ -TETA-OC and  $^{64}\text{Cu}$ -TETA-Y3-TATE. Receptor binding studies on CA20948 cell membranes showed highest affinities for TATE derivatives,  $^{64}\text{Cu}$ -TETA-Y3-TATE ( $0.308 \pm 0.0375$  nM) and  $^{64}\text{Cu}$ -TETA-TATE ( $0.297 \pm 0.0005$  nM), and lower affinities for  $^{64}\text{Cu}$ -TETA-OC ( $0.498 \pm 0.039$  nM) and  $^{64}\text{Cu}$ -TETA-Y3-OC ( $0.397 \pm 0.0206$  nM), suggesting that the C-terminal modification may contribute more to high-affinity receptor binding than the substitution at the 3-position. Similar trends were observed in cell uptake studies done with AR42J rat pancreatic tumor cells. These structure–activity relationship trends were not demonstrated in biodistributions in CA20948 tumor-bearing rats, but  $^{64}\text{Cu}$ -TETA-Y3-TATE exhibited tumor uptake 1.75–3.5 times higher than the other derivatives at 4 h postinjection (pi). These results reinforce the choice of  $^{64}\text{Cu}$ -TETA-Y3-TATE as the better PET imaging and targeted radiotherapy agent.

After demonstrating the superiority of CB-TE2A compared with TETA for stably chelating  $^{64}\text{Cu}$  *in vivo*,<sup>7</sup> we set out to attach CB-TE2A to the well-characterized tumor-targeting peptide, Y3-TATE. CB-TE2A was conjugated to the somatostatin analogue Y3-TATE and directly compared with the  $^{64}\text{Cu}$ -TETA-Y3-TATE conjugate.<sup>30</sup>  $^{64}\text{Cu}$ -CB-TE2A-Y3-TATE was radiolabeled in high radiochemical purity with specific activities of 1.3–5.1 mCi/ $\mu\text{g}$  of peptide at 95 °C and pH 8.0.<sup>31</sup> Biodistribution studies using AR42J tumors implanted in male Lewis rats revealed that this complex had greater affinity for somatostatin-positive tissues compared with the TETA conjugate. Accumulation of  $^{64}\text{Cu}$ -CB-TE2A-Y3-TATE was lower at all time points in blood and liver, and less accumulation was observed in the kidney at earlier time points compared with that of  $^{64}\text{Cu}$ -TETA-Y3-TATE. For example, the tumor to blood ratio at 4 h for  $^{64}\text{Cu}$ -CB-TE2A-Y3-TATE was  $156 \pm 55$ ; for  $^{64}\text{Cu}$ -TETA-Y3-TATE, the tumor to blood ratio was  $8.2 \pm 1.6$  ( $P < 0.001$ ). These data suggest that the  $^{64}\text{Cu}$ -CB-TE2A-Y3-TATE is more resistant to transchelation than the TETA analogue.

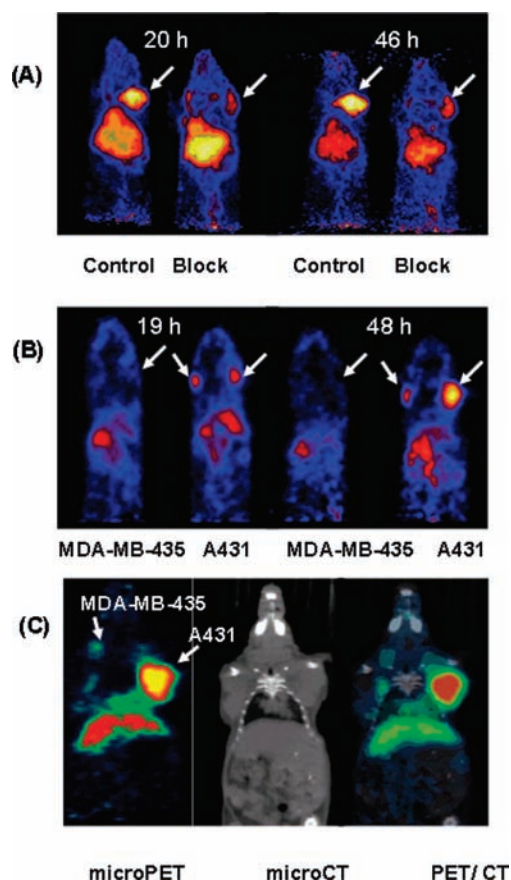


**FIGURE 6.** (A) Projection microPET images of A431 tumor-bearing nude mice 20 and 46 h postadministration of  $^{64}\text{Cu}$ -DOTA-cetuximab, with and without an injected blocking dose 20 h prior to the imaging dose (5.6 MBq, 6 g, left; 5.6 MBq, 1 mg of cetuximab, right). (B) Coronal microPET images of  $^{64}\text{Cu}$ -DOTA-cetuximab in A431 (epidermal growth-factor receptor [EGFR]-positive) and MDA-MB-435 (EGFR-negative) tumor-bearing mice 19 and 48 h postadministration of  $^{64}\text{Cu}$ -DOTA-cetuximab. (C) MicroPET/computed tomography co-registration images of  $^{64}\text{Cu}$ -DOTA-cetuximab in a mouse bearing both A431 and MDA-MB-435 tumors (arrow) at 24 h postinjection. Reprinted by permission of Mary Ann Liebert, Inc., from ref 38.

The majority of somatostatin analogs that have been evaluated for PET and SPECT imaging are somatostatin agonists, and as such, they are internalized into cells via receptor-mediated endocytosis and mimic the behavior of somatostatin itself. The pervasive belief has been that greater cellular internalization of a radiolabeled somatostatin analog *in vitro* is a predictor of improved tumor uptake *in vivo*. This has been demonstrated by the group at Rotterdam for  $^{111}\text{In}$ -labeled somatostatin analogs,<sup>32,33</sup> as well as by our group.<sup>28,30</sup> In 2006, Ginj et al. showed that an  $^{111}\text{In}$ -labeled somatostatin receptor type 2 (SSTR2) antagonist, sst2-ANT, had improved uptake compared with  $^{111}\text{In}$ -DTPA-Y3-TATE<sup>34</sup> in mice bearing SSTR2-transfected HEK cell tumors. The authors showed that sst2-ANT was not internalized in the HEK cells and dem-

onstrated classical antagonist behavior. We recently compared  $^{64}\text{Cu}$ -CB-TE2A-sst2-ANT with  $^{64}\text{Cu}$ -CB-TE2A-Y3-TATE in AR42J tumor-bearing rats.<sup>35</sup> In our hands,  $^{64}\text{Cu}$ -CB-TE2A-sst2-ANT showed low levels of internalization in AR42J cells, and similar uptake to  $^{64}\text{Cu}$ -CB-TE2A-Y3-TATE *in vivo* at early time points. An interesting characteristic of the SSTR2 antagonist is that it appears to bind to ~15-fold higher number of receptors than the agonist (23 000 vs 1551 fmol/mg protein), but with ~17-fold decreased affinity (26 vs 1.5 nM). However,  $^{64}\text{Cu}$ -CB-TE2A-sst2-ANT showed longer retention in the AR42J tumor, resulting in improved tumor/blood (72) and tumor/muscle (93) ratios at 24 h pi compared with  $^{64}\text{Cu}$ -CB-TE2A-Y3-TATE (tumor/blood = 20 and tumor/muscle = 45).<sup>35</sup>

### Targeting Epidermal Growth Factor Receptor (EGFR)

The epidermal growth factor family of membrane receptors is one of the most relevant targets in the tyrosine kinase family.<sup>36</sup> EGFR expression is increased in many human tumors such as breast cancer, squamous-cell carcinoma of the head and neck, and prostate cancer. Activation of EGFR contributes to several tumorigenic mechanisms, and in many tumors, EGFR expression may act as a prognostic indicator, predicting poor survival or more advanced disease stage.<sup>36</sup> At present, monoclonal antibodies (mAbs), which block the binding of EGF to the extracellular ligand-binding domain of the receptor, and small tyrosine kinase inhibitors have shown promise from a therapeutic standpoint. Cetuximab (C225, Erbitux) was the first mAb targeted against the EGFR approved by the Food and Drug Administration for the treatment of patients with EGFR-expressing metastatic colorectal carcinoma. Cetuximab binds to the extracellular domain of EGFR with a  $K_D$  of 1 nM, similar to that of the natural ligand, EGF.<sup>37</sup> We evaluated  $^{64}\text{Cu}$ -DOTA-cetuximab as a PET agent to image EGFRs in tumors.<sup>38</sup> For the cell binding affinity evaluation, highly EGFR-expressing human epithelial carcinoma A431 and low-expressing MDA-MB-435 melanoma cells were used. An equilibrium dissociation constant ( $K_D$ ) of 0.28 nM was obtained with the A431 cells, which was comparable to the literature reported values of unlabeled cetuximab with A431 cells.<sup>37</sup> The *in vivo* evaluation of  $^{64}\text{Cu}$ -DOTA-cetuximab was performed in A431 and MDA-MB-435 tumor-bearing mice. Both biodistribution and microPET data showed higher uptake in the EGFR positive A431 tumor than in the EGFR negative MDA-MB-435 tumor. Also, there was a reduced tumor uptake in A431 mice who received a blocking dose of unlabeled

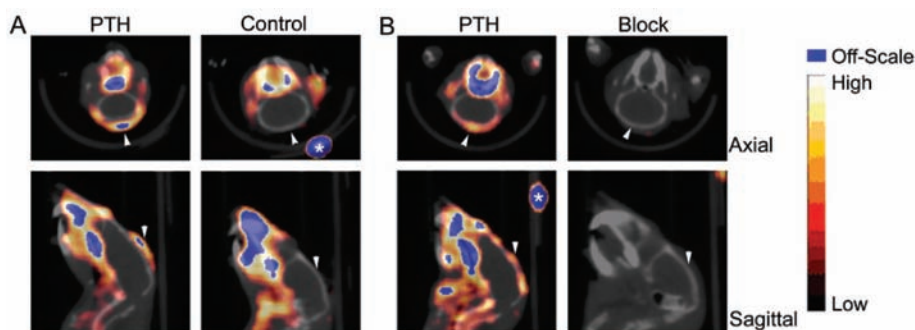


**FIGURE 7.** Small-animal PET/CT of PTH-treated mice. Calvarium uptake of  $^{64}\text{Cu}$ -CB-TE2A-c(RGDyK) was higher in PTH-treated mice (7.4 MBq [199  $\mu\text{Ci}$ ], 115 ng, SUV = 0.53) than in control mice (7.7 MBq [209  $\mu\text{Ci}$ ], 121 ng, SUV = 0.22) (A). In PTH-treated mice, uptake was reduced in all tissues, including calvarium, after injection of c(RGDyK) (PTH [left], 159  $\mu\text{Ci}$ , 84 ng, SUV = 0.33; block [right], 164  $\mu\text{Ci}$ , 87 ng, SUV = 0.18) (B). Arrowheads indicate calvarium of each animal. Fiducials (\*) are indicated. Reprinted by permission of the Society of Nuclear Medicine from ref 43.

cetuximab, demonstrating the specificity of  $^{64}\text{Cu}$ -DOTA-cetuximab for the high-EGFR-expressing A431 tumor (Figure 6).

The use of DOTA as the chelator with  $^{64}\text{Cu}$  is admittedly less than ideal. For this reason, metabolism experiments were performed to determine the extent of  $^{64}\text{Cu}$  transchelation to blood, liver, and tumor proteins in A431 tumor-bearing mice. The results showed minimal metabolism of  $^{64}\text{Cu}$ -DOTA-cetuximab in the blood out to 24 h pi. Liver metabolism studies demonstrated the transchelation of  $^{64}\text{Cu}$  to three proteins, two of which were shown by size-exclusion chromatography to be superoxide dismutase and metallothionein. The third metabolite was believed to be a protein aggregate. We are currently working on the development of CB macrocycles that can be labeled at lower temperatures (<43  $^{\circ}\text{C}$ ) and will be compatible with labeling of monoclonal antibodies, because we believe this will significantly improve retention of the agents in the liver, as well as possibly enhance tumor targeting.

$^{64}\text{Cu}$ -DOTA-cetuximab's potential to measure EGFR concentration was evaluated by PET imaging in cervical cancer tumors.<sup>39</sup> Overexpression of EGFR has been found in over 70% of carcinomas of the cervix. In this study,  $^{64}\text{Cu}$ -DOTA-cetuximab was used to correlate EGFR densities on the surface of five different cervical cancer lines with EGFR mRNA (mRNA) expression. Based on the cellular data, microPET imaging was performed on tumor-bearing mice using the highest-expressing cervical cancer cell line, CaSki. For the *in vitro* analysis, five cervical cancer cell lines were selected after a screen of 23 human cervical cancer lines based on their level of EGFR gene expression by gene expression microarray analysis. The five human tumor cell lines ranged in EGFR expression with the following order: CaSki (high), ME-180 and DcTc2 4510 (both midrange), HeLa (low), and C-33A (negative). The

cell-surface EGFR expression was evaluated by doing saturation binding assays at 4  $^{\circ}\text{C}$ , and the results paralleled the levels of EGFR expression determined by microarray analysis. *In vivo*, the biodistribution and small-animal PET studies with  $^{64}\text{Cu}$ -DOTA-cetuximab in CaSki human tumor-bearing nude mice showed relatively high tumor uptake at 24 h after injection (13.2% of injected activity per gram), with significant retention of radioactivity in blood and liver as well. Overall, the study evaluated  $^{64}\text{Cu}$ -DOTA-cetuximab as a biomarker of EGFR expression levels and a potential PET agent for patient selection and therapeutic monitoring.

### Targeting Integrin $\alpha_v\beta_3$

The integrin  $\alpha_v\beta_3$  is a well-known cell surface disease biomarker that is upregulated in tumor angiogenesis, metastasis, inflammation, certain cardiovascular abnormalities, and bone resorption.<sup>40</sup> There are many studies in the literature discussing PET imaging of  $\alpha_v\beta_3$  expression in tumor angiogenesis using arginine–glycine–aspartic acid (RGD) peptides.<sup>41</sup> As an alternative to imaging angiogenesis, we investigated imaging the upregulation of  $\alpha_v\beta_3$  in osteoclasts, which are present in high numbers in osteolytic bone metastases. Osteoclasts are known to have a high expression of  $\alpha_v\beta_3$  integrin compared with other normal cell types.<sup>42</sup> We proposed  $^{64}\text{Cu}$ -CB-TE2A-c(RGDyK) for detecting osteoclasts in osteolytic bone lesions.<sup>43</sup> Selective targeting of  $^{64}\text{Cu}$ -CB-TE2A-c(RGDyK) was demonstrated *ex vivo* in cell studies using  $\alpha_v\beta_5$ -positive bone marrow macrophages (BMM) and  $\alpha_v\beta_3$ -positive osteoclasts, with a maximal 2.6-fold increase in osteoclast uptake compared with BMM.

Since  $\alpha_v\beta_3$  is also expressed on many tumor cells, the osteoclast targeting by  $^{64}\text{Cu}$ -CB-TE2A-c(RGDyK) was validated *in vivo* in the absence of tumor cells by using a model of pharmacologically induced osteolysis. Parathyroid hormone (PTH)



induces osteoclast-mediated osteolysis when serially injected subcutaneously at the calvarium.<sup>44</sup> This pharmacologic model of PTH-induced osteolysis allowed investigation of osteoclast-mediated bone uptake independent of tumor cells. Increased uptake at the site of induced osteolysis was clearly visible on small animal PET as shown in Figure 7. In addition, the biodistribution studies demonstrated a significant increase in calvarium uptake in PTH-treated mice relative to controls. These results suggested the application of  $^{64}\text{Cu}$ -CB-TE2A-c(RGDyK) for imaging increased numbers of osteoclasts in osteolytic bone diseases. Efforts are ongoing in our lab to design improved targeting agents, both peptide-based and macromolecular, that target  $\alpha_v\beta_3$  for imaging tumor angiogenesis as well as increased numbers of osteoclasts in diseases that include osteolytic bone metastases.

## Conclusions

Copper-64-based radiopharmaceuticals have significant potential as oncological PET imaging agents. The longer half-life and ease of production of  $^{64}\text{Cu}$  by both reactor- and accelerator-based methods gives it a logistical and economical advantage over many positron-emitting radionuclides. The development of new BFC systems that form stable complexes with high kinetic inertness to Cu(II) decomplexation has proven valuable for producing favorable *in vivo* pharmacokinetic profile of peptide conjugates as demonstrated by the robust stability of  $^{64}\text{Cu}$ -CB-TE2A over traditionally used chelators such as DOTA and TETA. A better understanding of molecular markers has resulted in targeted imaging of tumors. The progress made at a fundamental level by using small animal PET systems will encourage the translation of  $^{64}\text{Cu}$ -based imaging radiopharmaceuticals into humans.

*The authors gratefully acknowledge NIH Grants R01 CA64475, R01 CA093375, R21 CA098698, and U01 HL080729-01.*

## BIOGRAPHICAL INFORMATION

**Monica Shokeen** is an Instructor in Radiology at Washington University School of Medicine. She received a B.S. (Honors) degree in Chemistry from the University of Delhi—New Delhi, India, in 1997, a M.B.A. degree from the Kurukshetra University, India, in 1999, and a Ph.D. in Inorganic Chemistry in 2006 from Washington University in St. Louis. Dr. Shokeen's research involves evaluation of small and macromolecular agents for molecular imaging and therapy of cardiovascular disease and cancer. She is also involved in imaging sciences based curriculum design and teaching.

**Carolyn J. Anderson** is a Professor of Radiology, Biochemistry & Molecular Biophysics, and Chemistry at Washington Univer-

sity in St. Louis. She received a B.S. degree in Chemistry from the University of Wisconsin—Superior in 1985 and a Ph.D. in Inorganic Chemistry from Florida State University in 1990. From 1990 to 1992, she was a postdoctoral research associate at the Mallinckrodt Institute of Radiology. In 1993, she was promoted to Assistant Professor of Radiology, and in 2007, she became full Professor of Radiology and Chemistry, followed by a joint appointment in Biochemistry and Molecular Biophysics in 2008. Prof. Anderson's research interests include the chelation chemistry of metal radionuclides and their attachment to tumor-targeting biomolecules for PET imaging of cancer and cancer metastasis.

## FOOTNOTES

\*To whom correspondence should be addressed. Mailing address: Mallinckrodt Institute of Radiology, Washington University School of Medicine, 510 S. Kingshighway Blvd., Campus Box 8225, St. Louis, MO 63110. Phone: 314-362-8427. Fax: 314-362-9940. E-mail: andersoncj@wustl.edu.

## REFERENCES

- Linder, M. C. *Biochemistry of Copper*; Plenum Press: New York, 1991; Vol. 10H.
- Frieden, E. Perspectives on copper biochemistry. *Clin. Physiol. Biochem.* **1986**, *4*, 11–19.
- Zinn, K. R.; Chaudhuri, T. R.; Cheng, T. P.; Morris, J. S.; Meyer, W. A. Production of no-carrier-added Cu-64 from zinc metal irradiated under boron shielding. *Cancer* **1994**, *73*, 774–778.
- Szelecsenyi, F.; Blessing, G.; Qaim, S. M. Excitation function of proton induced nuclear reactions on enriched  $^{61}\text{Ni}$  and  $^{64}\text{Ni}$ : Possibility of production of no-carrier-added  $^{61}\text{Cu}$  and  $^{64}\text{Cu}$  at a small cyclotron. *Appl. Radiat. Isot.* **1993**, *44*, 575–580.
- McCarthy, D. W.; Shefer, R. E.; Klinkowstein, R. E.; Bass, L. A.; Margeneau, W. H.; Cutler, C. S.; Anderson, C. J.; Welch, M. J. Efficient production of high specific activity  $^{64}\text{Cu}$  using a biomedical cyclotron. *Nucl. Med. Biol.* **1997**, *24*, 35–43.
- Cole, W. C.; DeNardo, S. J.; Meares, C. F.; McCall, M. J.; DeNardo, G. L.; Epstein, A. L.; O'Brien, H. A.; Moi, M. K. Serum stability of  $^{67}\text{Cu}$  chelates: Comparison with  $^{111}\text{In}$  and  $^{57}\text{Co}$ . *Nucl. Med. Biol.* **1986**, *13*, 363–368.
- Boswell, C. A.; Sun, X.; Niu, W.; Weisman, G. R.; Wong, E. H.; Rheingold, A. L.; Anderson, C. J. Comparative *in vivo* stability of copper-64-labeled cross-bridged and conventional tetraazamacrocyclic complexes. *J. Med. Chem.* **2004**, *47*, 1465–1474.
- Woodin, K. S.; Heroux, K. J.; Boswell, C. A.; Wong, E. H.; Weisman, G. R.; Niu, W.; Tomellini, S. A.; Anderson, C. J.; Zakharov, L. N.; Rheingold, A. L. Kinetic inertness and electrochemical behavior of Cu(II) tetraazamacrocyclic complexes: Possible implications for *in vivo* stability. *Eur. J. Inorg. Chem.* **2005**, *23*, 4829–4833.
- Busch, D. H. The complete coordination chemistry—One practitioner's perspective. *Chem Rev* **1993**, *93*, 847–860.
- Riesen, A.; Zehnder, M.; Kaden, T. A. Structure of the barium salt of a  $\text{Cu}^{2+}$  complex with a tetraaza macrocyclic tetraacetate. *Acta Crystallogr.* **1988**, *C44*, 1740–1742.
- Wu, Y.; Zhang, X.; Xiong, Z.; Chen, Z.; Fisher, D. R.; Liu, S.; Gambhir, S. S.; Chen, X. MicroPET imaging of glioma integrin  $\alpha_v\beta_3$  expression using  $^{64}\text{Cu}$ -labeled tetrameric RGD peptide. *J. Nucl. Med.* **2005**, *46*, 1707–1718.
- McQuade, P.; Miao, Y.; Yoo, J.; Quinn, T. P.; Welch, M. J.; Lewis, J. S. Imaging of melanoma using  $^{64}\text{Cu}$ - and  $^{86}\text{Y}$ -DOTA-ReCCMSH(Arg<sup>11</sup>), a cyclized peptide analogue of  $\alpha$ -MSH. *J. Med. Chem.* **2005**, *48*, 2985–2992.
- Chen, X.; Hou, Y.; Tohme, M.; Park, R.; Khankaldyyan, V.; Gonzales-Gomez, I.; Bading, J. R.; Laug, W. E.; Conti, P. S. Pegylated Arg-Gly-Asp peptide:  $^{64}\text{Cu}$  labeling and PET imaging of brain tumor  $\alpha_v\beta_3$ -integrin expression. *J. Nucl. Med.* **2004**, *45*, 1776–1783.
- Moi, M. K.; Meares, C. F.; McCall, M. J.; Cole, W. C.; DeNardo, S. J. Copper chelates as probes of biological systems: Stable copper complexes with a macrocyclic bifunctional chelating agent. *Anal. Biochem.* **1985**, *148*, 249–253.
- Anderson, C. J.; Pajean, T. S.; Edwards, W. B.; Sherman, E. L.; Rogers, B. E.; Welch, M. J. *In vitro* and *in vivo* evaluation of copper-64-octreotide conjugates. *J. Nucl. Med.* **1995**, *36*, 2315–2325.
- Anderson, C. J.; Jones, L. A.; Bass, L. A.; Sherman, E. L.; McCarthy, D. W.; Cutler, P. D.; Lanahan, M. V.; Cristel, M. E.; Lewis, J. S.; Schwarz, S. W. Radiotherapy, toxicity and dosimetry of copper-64-TETA-octreotide in tumor-bearing rats. *J. Nucl. Med.* **1998**, *39*, 1944–1951.

- 17 Bass, L. A.; Wang, M.; Welch, M. J.; Anderson, C. J. In vivo transchelation of copper-64 from TETA—octreotide to superoxide dismutase in rat liver. *Bioconjugate Chem.* **2000**, *11*, 527–532.
- 18 Weisman, G. R.; Rogers, M. E.; Wong, E. H.; Jasinski, J. P.; Paight, E. S. Cross-bridged cyclam. Protonation and Li<sup>+</sup> complexation in a diamond-lattice cleft. *J. Am. Chem. Soc.* **1990**, *112*, 8604–8605.
- 19 Weisman, G. R.; Wong, E. H.; Hill, D. C.; Rogers, M. E.; Reed, D. P.; Calabrese, J. C. Synthesis and transition-metal complexes of new cross-bridged tetraamine ligands. *Chem. Commun.* **1996**, 947–948.
- 20 Hubin, T. J.; McCormick, J. M.; Collinson, S. R.; Alcock, N. W.; Busch, D. H. Ultra rigid cross-bridged tetraazamacrocycles as ligands - the challenge and the solution. *Chem. Commun.* **1998**, 1675–1676.
- 21 Hubin, T. J.; Alcock, N. W.; Busch, D. H. The square-pyramidal PdII complex of a cross-bridged tetraazamacrocycle. *Acta Crystallogr.* **1999**, *C55*, 1404–1406.
- 22 Wong, E. H.; Weisman, G. R.; Hill, D. C.; Reed, D. P.; Rogers, M. E.; Condon, J. P.; Fagan, M. A.; Calabrese, J. C.; Lam, K.-C.; Guzei, I. A.; Rheingold, A. L. Synthesis and characterization of cross-bridged cyclams and pendant-armed derivatives and structural studies of their copper(II) complexes. *J. Am. Chem. Soc.* **2000**, *122*, 10561–10572.
- 23 Sun, X.; Wuest, M.; Weisman, G. R.; Wong, E. H.; Reed, D. P.; Boswell, C. A.; Motekaitis, R.; Martell, A. E.; Welch, M. J.; Anderson, C. J. Radiolabeling and in vivo behavior of copper-64-labeled cross-bridged cyclam ligands. *J. Med. Chem.* **2002**, *45*, 469–477.
- 24 Heroux, K. J.; Woodin, K. S.; Tranchemontagne, D. J.; Widger, P. C.; Southwick, E.; Wong, E. H.; Weisman, G. R.; Tomellini, S. A.; Wadas, T. J.; Anderson, C. J.; Kassel, S.; Golen, J. A.; Rheingold, A. L. The long and short of it: The influence of N-carboxyethyl versus N-carboxymethyl pendant arms on in vitro and in vivo behavior of copper complexes of cross-bridged tetraamine macrocycles. *Dalton Trans.* **2007**, 2150–2162.
- 25 Bauer, W.; Briner, U.; Doepfner, W.; Haller, R.; Huguénin, R.; Marbach, P.; Petcher, T. J.; Pless, J. SMS 201-995: A very potent and selective octapeptide analogue of somatostatin with prolonged action. *Life Sci.* **1982**, *31*, 1133–40.
- 26 Krenning, E. P.; Bakker, W. H.; Kooij, P. P.; Breeman, W. A.; Oei, H. Y.; de Jong, M.; Reubi, J. C.; Visser, T. J.; Bruns, C.; Kwekkeboom, D. J.; et al. Somatostatin receptor scintigraphy with indium-111-DTPA-D-Phe-1-octreotide in man: Metabolism, dosimetry and comparison with iodine-123-Tyr-3-octreotide. *J. Nucl. Med.* **1992**, *33*, 652–658.
- 27 Anderson, C. J.; Dehdashti, F.; Cutler, P. D.; Schwarz, S. W.; Laforest, R.; Bass, L. A.; Lewis, J. S.; McCarthy, D. W. <sup>64</sup>Cu-TETA-octreotide as a PET imaging agent for patients with neuroendocrine tumors. *J. Nucl. Med.* **2001**, *42*, 213–221.
- 28 Lewis, J. S.; Lewis, M. R.; Srinivasan, A.; Schmidt, M. A.; Wang, J.; Anderson, C. J. Comparison of four <sup>64</sup>Cu-labeled somatostatin analogues in vitro and in a tumor-bearing rat model: Evaluation of new derivatives for positron emission tomography imaging and targeted radiotherapy. *J. Med. Chem.* **1999**, *42*, 1341–1347.
- 29 de Jong, M.; Breeman, W. A.; Bakker, W. H.; Kooij, P. P.; Bernard, B. F.; Hofland, L. J.; Visser, T. J.; Srinivasan, A.; Schmidt, M. A.; Erion, J. L.; Bugaj, J. E.; Macke, H. R.; Krenning, E. P. Comparison of (111)In-labeled somatostatin analogues for tumor scintigraphy and radionuclide therapy. *Cancer Res.* **1998**, *58*, 437–441.
- 30 Sprague, J. E.; Peng, Y.; Sun, X.; Weisman, G. R.; Wong, E. H.; Achilefu, S.; Anderson, C. J. Preparation and biological evaluation of copper-64-labeled Tyr3-octreotate using a cross-bridged macrocyclic chelator. *Clin. Cancer Res.* **2004**, *10*, 8674–8682.
- 31 Wadas, T. J.; Anderson, C. J. Radiolabeling of TETA- and CB-TE2A-conjugated peptides with copper-64. *Nat. Protoc.* **2006**, *1*, 3062–3068.
- 32 de Jong, M.; Bakker, W. H.; Krenning, E. P.; Breeman, W. A.; van der Pluijm, M. E.; Bernard, B. F.; Visser, T. J.; Jermann, E.; Behe, M.; Powell, P.; Macke, H. R. Yttrium-90 and indium-111 labelling, receptor binding and biodistribution of [DOTA0,d-Phe1, Tyr3]octreotide, a promising somatostatin analogue for radionuclide therapy. *Eur. J. Nucl. Med.* **1997**, *24*, 368–371.
- 33 de Jong, M.; Bernard, B. F.; de Bruin, E.; van Gameren, A.; Bakker, W. H.; Visser, T. J.; Maecke, H. R.; Krenning, E. P. Internalization of radiolabelled [DTPA0]octreotide and [DOTA0, Tyr3]octreotide: Peptides for somatostatin receptor-targeted scintigraphy and radionuclide therapy. *Nucl. Med. Commun.* **1998**, *19*, 283–288.
- 34 Ginj, M.; Zhang, H.; Waser, B.; Cescato, R.; Wild, D.; Wang, X.; Erchegyi, J.; Rivier, J.; Macke, H. R.; Reubi, J. C. Radiolabeled somatostatin receptor antagonists are preferable to agonists for in vivo peptide receptor targeting of tumors. *Proc. Natl. Acad. Sci. U.S.A.* **2006**, *103*, 16436–16441.
- 35 Wadas, T. J.; Eiblmaier, M.; Zheleznyak, A.; Sherman, C. D.; Ferdani, R.; Liang, K.; Achilefu, S.; Anderson, C. J. Preparation and biological evaluation of <sup>64</sup>Cu-CB-TE2A-sst2-ANT, a somatostatin antagonist for PET imaging of somatostatin receptor-positive tumors. *J. Nucl. Med.* **2008**, *49*, 1819–1827.
- 36 Laskin, J. J.; Sandler, A. B. Epidermal growth factor receptors: A promising target in solid tumors. *Cancer Treat. Rev.* **2004**, *30*, 1–17.
- 37 Fan, Z.; Masui, H.; Altas, I.; Mendelsohn, J. Blockage of epidermal growth factor receptor function by bivalent and monovalent fragments of C225 anti-epidermal growth factor receptor monoclonal antibodies. *Cancer Res.* **1993**, *53*, 4322–4328.
- 38 Li, W. P.; Meyer, L. A.; Capretto, D. A.; Sherman, C. D.; Anderson, C. J. Receptor-binding, biodistribution, and metabolism studies of <sup>64</sup>Cu-DOTA-cetuximab, a PET-imaging agent for epidermal growth-factor receptor-positive tumors. *Cancer Biother. Radiopharm.* **2008**, *23*, 158–171.
- 39 Eiblmaier, M.; Meyer, L. A.; Watson, M. A.; Fracasso, P. M.; Pike, L. J.; Anderson, C. J. Correlating EGFR expression with receptor-binding properties and internalization of <sup>64</sup>Cu-DOTA-cetuximab in 5 cervical cancer cell lines. *J. Nucl. Med.* **2008**, *49*, 1472–1479.
- 40 Hood, J. D.; Cheresch, D. A. Role of integrins in cell invasion and migration. *Nat. Rev. Cancer* **2002**, *2*, 91–100.
- 41 Haubner, R.; Decristoforo, C. Radiolabelled RGD peptides and peptidomimetics for tumour targeting. *Front. Biosci.* **2009**, *14*, 872–886.
- 42 Horton, M. A. The alpha v beta 3 integrin “vitronectin receptor”. *Int. J. Biochem. Cell Biol.* **1997**, *29*, 721–725.
- 43 Sprague, J. E.; Kitaura, H.; Zou, W.; Ye, Y.; Achilefu, S.; Weilbaecher, K. N.; Teitelbaum, S. L.; Anderson, C. J. Noninvasive imaging of osteoclasts in parathyroid hormone-induced osteolysis using a <sup>64</sup>Cu-labeled RGD peptide. *J. Nucl. Med.* **2007**, *48*, 311–318.
- 44 Yates, A. J.; Gutierrez, G. E.; Smolens, P.; Travis, P. S.; Katz, M. S.; Aufdemorte, T. B.; Boyce, B. F.; Hymer, T. K.; Poser, J. W.; Mundy, G. R. Effects of a synthetic peptide of a parathyroid hormone-related protein on calcium homeostasis, renal tubular calcium reabsorption, and bone metabolism in vivo and in vitro in rodents. *J. Clin. Invest.* **1988**, *81*, 932–938.
- 45 Jones-Wilson, T. M.; Deal, K. A.; Anderson, C. J.; McCarthy, D. W.; Kovacs, Z.; Motekaitis, R. J.; Sherry, A. D.; Martell, A. E.; Welch, M. J. The in vivo behavior of copper-64-labeled azamacrocyclic compounds. *Nucl. Med. Biol.* **1998**, *25*, 523–530.